This full text paper was peer-reviewed at the direction of IEEE Instrumentation and Measurement Society prior to the acceptance and publication.

978-1-5386-2092-2/18/$31.00 ©2018 IEEE

Design and implementation of a microsensor platform for protein detection realized via 3-D printing

Andrea Bodini, Edoardo Cantu', Mauro Serpelloni, Emilio Sardini, Sarah Tonello
Department of Information Engineering
University of Brescia
Brescia, Italy
sarah.tonello@unibs.it

***Abstract*—The possibility to implement engineered devices to obtain feedbacks from biological samples represent a powerful approach to bring significant improvement in diagnostics and biotechnological research. Among several 3D printing techniques, Aerosol Jet Printing (AJP) appears really promising for this kind of applications. Its main benefits are related to manufacturing of customized, complex geometries with a high resolution even on irregular surfaces. In this paper, we present the realization of an Aerosol Jet Printed microdevice addressed to protein detection and quantification in biological samples. The device was manufactured with particular attention to materials and geometry choices. A profilometer analysis was at first performed to determine the thickness of printed layers. Then electric tests were performed, to evaluate the electrical resistance offered by the printed elements. Finally, the possibility to immobilize antibodies on the sensor to perform protein quantification was assessed with fluorescence imaging. Results obtained confirmed the possibility to print with AJP high resolution lines, with proper values of resistivity. In conclusion, imaging findings suggested a good adhesion of antibodies on the electrodes, confirming the designed sensors as promising candidates for the electrochemical analysis of biological samples fluids.**

Keywords—microsensor; protein detection; 3-D printing; aerosol jet printing.

I. INTRODUCTION

The definition of additive manufacturing (AM) given by the American Society for Testing Materials (ASTM) International Committee on Additive Manufacturing Technologies [1] defines the process of joining materials to make objects from 3D model data, usually layer upon layer. AM follows the popularisation of 3D solid modelling Computer Aided Design (CAD) [2].

Born in America in the late 1930's, AM is commonly considered the greatest achievement in the recent 30 years in manufacturing field and today it is a core technology in international industry ,leading the process known as "third industrial revolution" [3].

Several fields of engineering (e.g. aerospace, automotive, biomedical) benefit from the ability of AM to shape complex geometries with a high resolution and to customize the design for each specific need. Automotive industry has sped up product development [2], while, in the medical field, orthopaedic and dental implants [4] benefit significantly from the ability to make rough, engineered surface for more effective bone integration.

Several distinguished companies (e.g. CRP technology, OPTOMEC) has emerged to promote interesting AM applications ranging from the realization of components for motorsport to complex structural and functional components for satellites, helicopters, jet engines, or vehicle, publishing specific patents for the implemented fabrication techniques.

Printed electronics represents another attractive and innovative field of application of AM. Flexible electronic devices, paper electronics and wearable devices are now widespread, so there is an urgent need for advanced printing processes, reducing the number of processing steps, material waste and production cost. Several significant examples can be highlighted in the literature. Among them the development of aerosol-assisted atmospheric pressure plasma-based process represent an interesting solution aiming to rapid and cost-effective printing technology. Site-selective deposition of materials, the ability to perform encapsulation, integration of the process, and good mechanical flexibility of the printed substrates without loss of functionality are attractive features of this highly versatile technique [6]. Further, another promising example of this application field was developed by Li et al.. who developed a transparent, mechanically flexible, and thermally stable electrolyte with high capacitance by exploiting the potential of 3D printing for curing printed resin and ionic liquid composite at high temperature [7].

In addition to its most traditional applications, printed electronics has emerging as promising candidate in fields like diagnostics or tissue engineering. Here, the production of technological platforms able to give feedbacks on biological samples or physiological processes is the key for improving available assays. Moreover, the recent attention for disposable, low-cost and reliable biomolecule-to-chip interface systems for high-throughput in-vitro toxicity assays and pharmacology, is becoming a urgent need due to novel international regulatory guidelines[8].

Methods such as screen printing or ink-jet printing are most frequently selected for these applications. Several examples of

electrochemical sensors for biotechnological applications produced with these techniques can be found in the literature, going from chemicals detection to DNA or protein recognition [9], [10]. These two techniques have been also combined, as showed by Kit-Anan et al. [11] who succeeded in detect ascorbic acid with a disposable paper-based electrochemical sensor fabricated using screen-printing for base material and inkjet-printing for modifying functional material. Hu et al. [12] developed a method to fabricate hundreds of nano-porous gold electrode arrays on cellulose membranes for electrochemical oxygen sensing, using ionic liquid (IL) electrolytes with an inexpensive inkjet printer.

Considering all the benefits described above, 3D printing has been recently considered as a potential candidate to bring the production of biosensors to a next level in term of resolution, customization, standardization, aiming to innovate and improve the performances of the traditional techniques [13], [14].

In light of this, the present work aims to propose the use of a relatively new AM technique, Aerosol Jet Printing (AJP), to realize a customized measuring device with electrochemical sensors, addressable for the analysis of biological samples.

In section two, an overview on the AJP method will be presented, focusing the attention to the physics of this technique. Section three will present the detailed methods followed for device fabrication, with a particular attention to inks and printing conditions. Finally, preliminary results related to sensors geometrical and electrical features, together with an evaluation of the device compatibility with diagnostic assay routine will be presented in section four.

II. Aerosol Jet Printing

A. Introduction to AJP

AJP is a quite novel additive manufacturing technique belonging to material jetting family. It generates liquid droplets, which are deposited on the working platform to partially soften the previous layer of material and solidify as one piece during the process [15]. AJP belongs to Aerosol-based direct-write (A-DW) family, a subset of droplet-based direct-write: an aerosol beam is gathered and directed toward a substrate to realize specific surface features (e.g., dots or lines) without using masks or post-patterning (i.e., laser trimming) [16]. Aerosol Jet was formerly referred to as M^3D (maskless mesoscale materials deposition) and was developed by Optomec under the Defense Advanced Research Projects Agency (DARPA) Mesoscopic Integrated Conformal Electronics (MICE) program. The commercially available system prints traces from 10 μm to 5mm in width at translation speeds up to 200 mm/s. The liquid inks used typically have a viscosity between 0,5 and 2500cP. Fig. 1 represents the deposition phase using AJP.

Aerosol Jet has been used to successfully demonstrate many advanced applications, like high-efficiency solar and fuel cells, EMI shielding, fully-printed thin-film transistors, embedded resistors, antennae, sensors, flexible displays and circuitry, high-density assays for drug discovery [17].

B. Functioning of Aerosol Jet Printing

Aerosol jet printing is a four-step process [18]:

- Atomization of the ink;
- Densification of the generated aerosol;
- Focusing of the aerosol;
- Deposition of the droplets on the substrate.

The aerosol is generated starting from an ink or dispersion by a pneumatic Collison atomizer, with the usage of a carrier gas, typically nitrogen or compressed dry air. The dynamic viscosity of the ink must be about η=1—1000 mPa·s and in some cases it is necessary to densify the aerosol. In light of this, superfluous carrier gas have to be removed and the aerosol droplet size distribution to be adjusted, thanks to a virtual impactor, which increases the volume fraction of the aerosol droplet flow. The typical setup allows the production of droplets smaller than 5 µm in diameter. As presented in fig. 2, the aerosol is focused in the print head: in its centre the aerosol flow is directed into the transition region, where a sheath gas surround cylindrically the flow. Following, the gaseous complex is accelerated when entering the print nozzle, thus to reach at the nozzle exit an inner radius inferior than 50 mm. The sheath gas is important because it prevents possible droplets' impacts or condensation of solvents from the aerosol at the inner wall of the nozzle and it drives the aerosol flow. Increasing the sheath gas flow additionally, the aerosol diameter can be reduced. The droplets, thanks to their high momentum, do not change their own direction, following the gas flow at the sample surface, and impact the substrate (two to five millimeters below the nozzle exit, with the surface perpendicular to it), which may be heated to evaporate deposited solvents.

III. Sensor Fabrication

Optomec's Aerosol Jet Printing AJ300 system was employed in the realization of our device: this 3D printing machine is designed to interface with AutoCAD drawings.

A. Sensor design

Considering printed electrodes already present on the market (fig. 3a) and other works in the literature [19], sensors final

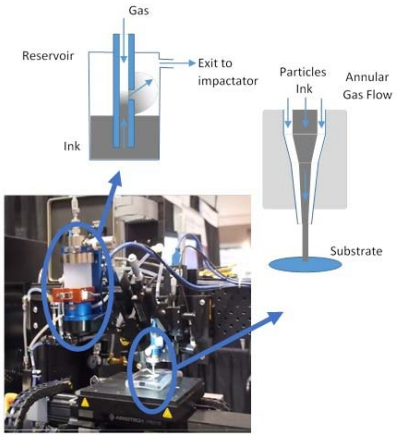

Fig. 1. Deposition phase scheme for Aerosol Jet Printing.

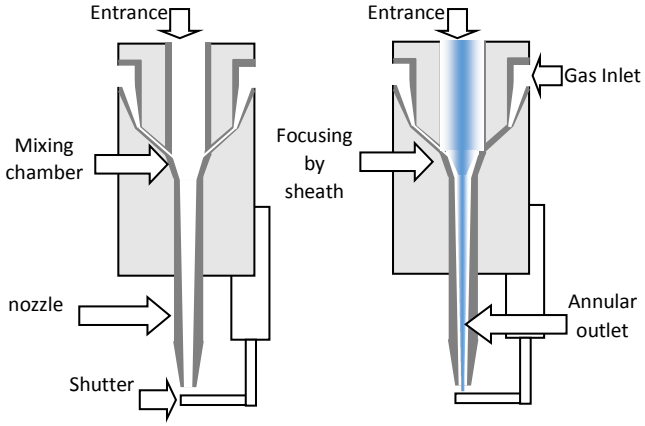

Fig. 2. Schematic of an aerosol jet print head.

layout was designed using the 3-electrodes system (working (WE), counter (CE) and reference (RE) electrodes) commonly adopted for electrochemical measurements (fig. 3).The same geometry was reproduced, on the same substrate, scaled in four different dimensions, with a diameter of WE of 4 mm, 3 mm, 2 mm and 1mm respectively. Three sensors for each geometry were printed, in order to obtain a good repeatability (fig. 4) and to choose the dimension in order to reduce the noise and the interference from currents due to electrolytic buffer and to highlight the signal due to analyte presence in the post-processing analysis. During the design phase, particular attention was put in selecting the proper thickness of the drawing lines and the distances between them, so that, tuning printer parameters according to ink viscosity, a homogeneous filling of the electrodes and pads could be ensured. Further, a devoted Optomec's gadget for AutoCAD was used to ensure a proper ink filling of closed shapes. Moreover, all the lines were designed as polylines, in order to improve the timing and the homogeneity of printed lines (Red lines in fig.4).

The drawing presented in fig. 4 shows all the layers corresponding to the different employed inks: silver (in yellow) for the conductive tracks, carbon (in black) for WE and CE, silver chloride (in white) for RE and polyimide (in orange) for creating a sort of delimiting wall to help containing water-based samples. The general design proposed might be customized through a proper functionalization with biomolecules that will ensure the specificity for the target analyte.

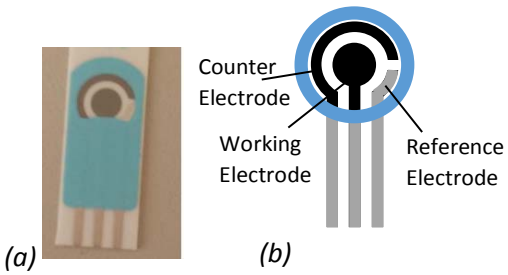

Fig. 3. (a) a commercial sensor; (b) conceptual drawing developed by Gang et al [19].

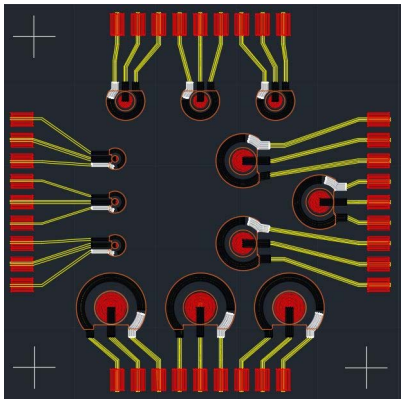

Fig. 4. AutoCAD drawing of our prototype.

B. *Materials*

Alumina was selected as optimal substrate, due to its mechanical properties and its porosity, which ensures a proper ink adhesion. Glass was as well considered as potential substrates.

The details of the four inks used for sensors production are following discussed. Silver ink is produced by UTDots Inc., with its own thinner, UTDAg ink is based on silver nanoparticles with average size around 10 nm and dispersed in a liquid vehicle. Nanosilver concetration is about 25-60wt%, with a viscosity of 1-30 cP. Since they are surface stabilized, UTDAg inks are highly soluble in nonpolar organic solvents and stable under atmospheric conditions at room temperature. Silver chloride ink was purchased by Fujikura Kasei. Co. Ltd. together with its own thinner. It is possible to find this ink in different weight proportion of Ag/AgCl ratios: the one we employed was characterized by a ratio of 8/2. Since the ink starting viscosity was 300±50 dPa·s, it was necessary to dilute the ink with its thinner before printing, following the equations present in the literature regarding a two-component blend [20]. Carbon ink was purchased by Creative Materials Inc., characterized by a starting viscosity of 15-20Pa·s. Polyimide ink is produced by HD MicroSystems Inc., it belongs to PI-2500 series, a family of polyimides which imidizes faster and at lower temperatures (200 °C) than standard polyimide precursors.

C. *Printing and sintering phase*

In order to reach the proper viscosity, each ink was properly tuned with its own thinner and these two parts were placed in our Optomec's AJ300 printing machine.

Each ink was printed considering its own specific process parameters, reported in Table I.

After the printing step, each ink was cured in oven:

- Silver was cured at 220 °C per 10 minutes;
- Carbon was cured at 115 °C per 5 minutes;
- Silver chloride was cured at 120 °C per 30 minutes;
- Polyimide was cured at 120 °C per 20 minutes.

Examples of the printed sensors on the alumina substrate are reported in fig. 5.

TABLE I. PRINTING PROCESS PARAMETERS

Process Parameters	Materials			
	Ag	*AgCl*	*C*	*PI*
Sheath gas flow (SCCM)	50	130	40	150
Exhaust flow (SCCM)	830	600	1000	1300
Atomizer flow (SCCM)	810	550	900	1270
Process speed (mms-1)	2	2	2	3
Plate temperature (°C)	60	65	75	70

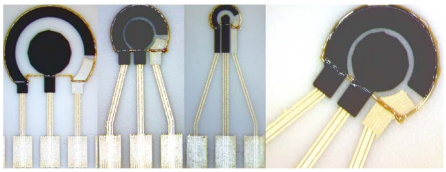

Fig. 5 Examples of the printed sensors on the alumina substrate, from left to right: 4 mm,3 mm,1 mm and 2 mm geometries.

IV. PRELIMINARY RESULTS

In order to evaluate the possibility to apply the device in experiments for proteins detection in biological samples, different aspects of the sensors were investigated.

At first, an analysis of the geometrical and electrical parameters was performed in order to fully characterize the sensors. After that, it was evaluated more properly the compatibility of the sensors with wet lab practises involved in the assays for protein quantification. Thus, sample volume amount was investigated and after that, the effective coating of antibodies was assessed using fluorescence imaging.

A. Geometric analysis

1) Methods

The profilometer used in this work is an Alpha-Step IQ Kla Tencor, a diamond stylus- based system for step height measurements, with a range 8 nm – 2 mm, with an uncertainty of 0.1%.

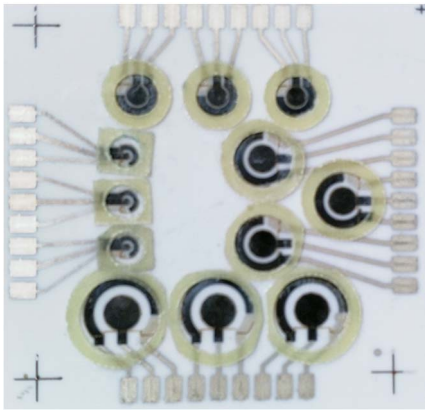

Fig. 6. Printed circuits modified with glass fiber washers.

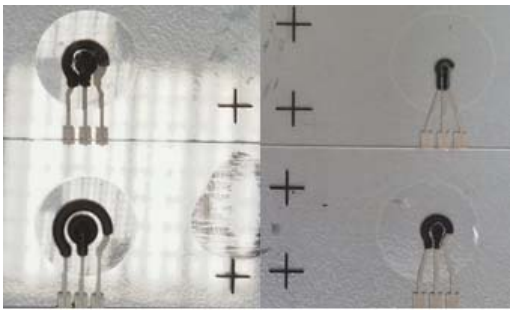

Fig. 7. Picture of the circuits printed on glass.

The system is provided of an integrated optical microscope which allows an automatized selection of the region of interest. The maximum length of the profile is 2 mm. The stylus speed can be tuned between 2 and 200 µm/s. The bending radius (nominal) of the diamond tip is 5 µm. Data are recorded and can be analyzed in real time by a dedicated software.

For sensors analysis, a testing force of $62x10^{-6}$ N was considered. Our interest was to determine the thickness of printed lines for each type of ink and, for the overall circuit, to know the total area covered by the paths. The total area was evaluated as a sum of consecutive trapezoid areas.

The process parameters considered in this phase were:

- Scan speed: 50 $\mu ms^{-1}$for PI, 20 $\mu ms^{-1}$for Ag, AgCl and C;
- Scan length: 1000 µm;
- Sampling rate: 50 Hz.

TABLE II. THICKNESS AND SECTIONS OF DEPOSITIED INKS

Material	*Thickness (µm)*	*Standard Deviation*	*Section (μm^2)*
Ag	6.8	±1	854.2
AgCl	4	±1	392.3
C	6.5	±0.2	365.3
PI	2.7	±2	/

1) Results

In Table II it is possible to see thickness and section data obtained with the abovementioned process parameters of the printed lines for each ink. In synthesis, results obtained allow to state that the paths have a congruent thickness with the nominal values stated in the datasheet of the Optomec Printing System (single layer thickness in the range 100 nm to 10 um). The differences between the results obtained for each ink can be interpreted and compared taking into account different process parameters, number of printed layers and further considering viscosity: higher thicknesses were obtained for inks with higher viscosity.

B. Electrical resistance

1) Methods

Electrical resistance of the printed paths was measured using a digital bench-top multimeter (Hewlett-Packard 34401a). During these experiments, testing probes were applied to the

extremities of each path, thus measuring the resistance offered by all its length. At first, the resistance of pure inks deposited printing sample geometries was evaluated, then resistance of each electrodes on the printed sensors with the final layout was measured. This allowed to compare resistivity values of each ink's datasheet with the ones obtained during tests and to evaluate the contribute of each material in the complete sensor. For each element, ten measures have been performed, calculating then mean values and standard deviations.

Once these values were obtained, it was possible to get resistivity considering the definition of resistance:

$$R=\rho \cdot l \cdot S^{-1}, \quad (1)$$

Where R is resistance, ρ is resistivity, *l* is the length of the considered path and *S* its section.

2) Results

In Table III it is possible to find measured resistance and calculated resistivity data of pure printed inks, while table IV presents the same data for the printed sensors. Data presented in table III appeared in agreement with the nominal values of the manufacturers, taking into account the specific process parameters.

More in detail, Ag experimental resistivity ($12{,}2\cdot10^{8}$ Ωm) can be compared with the nominal one ($3\cdot10^{-8}$ Ωm), considering as most relevant affecting variables the substrate (ceramic and glass are not the optimal indicated by UTDots). AgCl experimental resistivity value ($71{,}3\cdot10^{-8}$ Ωm) can be compared with the nominal one reported by Fujikura Kasei. Co. Ltd ($56\cdot10^{-8}$ Ωm), considering the use of the thinner to achieve the viscosity required for printing. Finally, C experimental resistivity ($159{,}6\cdot10^{-8}$ Ωm) appear increased compared to the theorical one given by Creative Materials ($3\cdot10^{-8}$ Ωm), probably due to the usage of a non-optimal substrate and due to different post-processing parameters.

TABLE III. RESISTANCE AND RESISTIVITY OF DEPOSITIED INKS

Material			
	Resistance (Ω)	***Path length (mm)***	***Resistivity (Ωm)***
Ag	1,6±0,4	11	$12{,}2\cdot10^{-8}$
AgCl	21,0±1,3	12	$71{,}3\cdot10^{-8}$
C	84,3±4,9	12.5	$159{,}6\cdot10^{-8}$

TABLE IV. RESISTANCE AND RESISTIVITY OF PRINTED SENSORS

WE diameter			
	Resistance (Ω)	***Path length (mm)***	***Resistivity (Ωm)***
4mm	7,3±1,8	11	$53{,}0\cdot10^{-8}$
3mm	5,8±1	10	$32{,}1\cdot10^{-8}$
2mm	5,7±0,42	11	$14{,}0\cdot10^{-8}$

Fig. 8. Different drops deposited on the biggest sensors.

TABLE V. WORKING VOLUMES

Sensor dimension	***WE volume (µl)***	***Measurement volume (µl)***
4 mm	18	60
3 mm	12	20
2 mm	7	15
1 mm	2	3-4

C. Sample volume optimization

1) Methods

The first test performed was the definition of the optimal volumes (measured as amount of liquid, in µl) that each geometry could hold (fig. 8). This test involved previously only the WE, to optimize the amount of volume for each step of the biofunctionalization, and then all three electrodes, to optimize the optimal volume for the final measurement.

Using a micropipette, different volumes of Phosphate Buffered Saline (PBS) from (Sigma Aldrich) were dropped, in order to optimize the values for future tests with biological samples.

2) Results

In Table V the working volumes obtained during sample amount quantification are summarized, for each different geometry, both for functionalization and for measurements.

D. Fluorescence imaging

1) Methods

After optimizing working volumes, the effectiveness of primary antibodies coating on the carbon WE was evaluated using a near infra-red imaging system (Odyssey® Fc Dual-Mode Imaging System from LI-COR Biosciences). This test is required to ensure a proper electrodes biofunctionalization for protein quantification. More specifically, biomolecules adhesion onto carbon WE were qualitatively detected by labelling each antibody with a fluorescent tag, and then recording the emitted light in the near infrared region using the Odyssey intensity quantifier.

A coating with an 8 µl/ml solution of anti-interleukin 8 primary antibody (Duo Set kit) was performed, dropping with a micropipette the volumes previously optimized, proportionally to the size of the various circuits. Two electrodes were kept as control (blank samples), covered with pure PBS solution. After that, sensors were placed in a humid chamber prepared through a box and wet paper to avoid solution evaporation and incubated for a night at 4 °C.

The next day, after washing with a solution of PBS with 0.05% Tween, sensors were incubated with a solution of secondary antibodies, labelled with a fluorescent tag functional for the final imaging with Odyssey system. After two hours, according to its protocol of use, sensors were washed and imaged. More

specifically, sensors were excited with a 685nm light source and the emitted light in the near infrared region was measured with the Odyssey LI-COR system, in order to reveal the coating deposition.

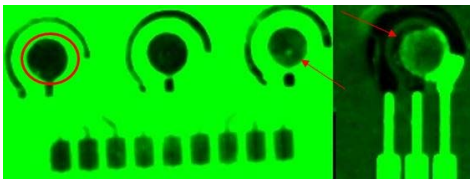

Fig. 9. A glass-substrate sensor, to the right, and three alumina-substrate sensors, to the left, covered by protein.

1) Results

Results obtained showed a clear difference between blank electrodes (black in the image, not emitting any light) and antibodies coated ones (appearing as a clearer emitting spot in the image), as shown in fig. 9. The red arrows indicate the zones successfully covered by antibodies.

These findings confirmed the possibility to use these materials and AJP technique to produce electrodes, which allow a homogeneous adhesion of antibodies, essential to perform a complete functionalization to perform immune-sensing of proteins. The homogeneous deposition of primary antibodies would allow a more effective quantification of proteins, thus reducing the interference of currents due to un-specific adsorption.

V. Conclusions

In this paper, we have reported the realization of a microsensor platform for protein detection, developed through the usage of a quite novel 3D printing technique: Aerosol Jet Printing. Electrodes and conductive tracks with a high resolution and controllable thickness could be realized using this technique, showing proper values of electrical resistivity coherent with each ink. Furthermore, antibodies have shown good adhesion to the sensors on both the employed substrates.

In light of this, future studies will test the capability of our sensors to trace the presence of proteins in different biological samples.

Furthermore, future development might focus on the reproduction of similar geometries, with optimized parameters, on different biocompatible materials for the substrate, such as soft materials (e.g. PDMS), varying their geometry to achieve the same containment effect of glass slides concavity and of glass fiber washers glued on alumina.

Acknowledgment

The authors would like to acknowledge Giulia Abate and Mariagrazia Marziano for providing biological materials for sensors characterization and for precious collaboration during these experiments, and Maurizio Donarelli for his help in performing the profilometer tests.

References

[1] Wohlers Report 2015, 3D Printing and Additive Manufacturing State of the Industry, Annual Worldwide Progress Report. 2015.

[2] I. Gibson, “The changing face of additive manufacturing,” J. Manuf. Technol. Manag., vol. 28, no. 1, pp. 10–17, 2017.

[3] L. Chen, Y. He, Y. Yang, S. Niu, and H. Ren, “The research status and development trend of additive manufacturing technology,” Int. J. Adv. Manuf. Technol., vol. 89, no. 9–12, pp. 3651–3660, 2017.

[4] N. Guo and M. C. Leu, “Additive manufacturing: Technology, applications and research needs,” Front. Mech. Eng., vol. 8, no. 3, pp. 215–243, 2013.

[5] “CRP Technology.” .

[6] R. P. Gandhiraman, V. Jayan, J. W. Han, B. Chen, J. E. Koehne, and M. Meyyappan, “Plasma jet printing of electronic materials on flexible and nonconformal objects,” ACS Appl. Mater. Interfaces, vol. 6, no. 23, pp. 20860–20867, 2014.

[7] H. Li, Y. Tang, W. Guo, H. Liu, L. Zhou, and N. Smolinski, “Polyfluorinated Electrolyte for Fully Printed Carbon Nanotube Electronics,” Adv. Funct. Mater., vol. 26, no. 38, pp. 6914–6920, 2016.

[8] A. Spanu, S. Lai, P. Cosseddu, M. Tedesco, S. Martinoia, and A. Bonfiglio, “An organic transistor-based system for reference-less electrophysiological monitoring of excitable cells,” Sci. Rep., vol. 5, p. 8807, Mar. 2015.

[9] R. A. S. Couto, J. L. F. C. Lima, and M. B. Quinaz, “Recent developments, characteristics and potential applications of screen-printed electrodes in pharmaceutical and biological analysis,” Talanta, vol. 146, pp. 801–814, Jan. 2016.

[10] J. Li, F. Rossignol, and J. Macdonald, “Inkjet printing for biosensor fabrication: combining chemistry and technology for advanced manufacturing,” Lab Chip, vol. 15, no. 12, pp. 2538–2558, 2015.

[11] W. Kit-Anan et al., “Disposable paper-based electrochemical sensor utilizing inkjet-printed Polyaniline modified screen-printed carbon electrode for Ascorbic acid detection,” J. Electroanal. Chem., vol. 685, pp. 72–78, 2012.

[12] C. Hu, X. Bai, Y. Wang, W. Jin, X. Zhang, and S. Hu, “Inkjet printing of nanoporous gold electrode arrays on cellulose membranes for high-sensitive paper-like electrochemical oxygen sensors using ionic liquid electrolytes,” Anal. Chem., vol. 84, no. 8, pp. 3745–3750, 2012.

[13] H. Ragones et al., “Disposable electrochemical sensor prepared using 3D printing for cell and tissue diagnostics,” Sensors Actuators B Chem., vol. 216, no. Supplement C, pp. 434–442, 2015.

[14] H. Yang, T. Rahman, D. Du, R. Panat, and Y. Lin, “3-D Printed Adjustable Microelectrode Arrays for Electrochemical Sensing and Biosensing.,” Sens. Actuators. B. Chem., vol. 230, pp. 600–606, Jul. 2016.

[15] J.-Y. Lee, J. An, and C. K. Chua, “Fundamentals and applications of 3D printing for novel materials,” Appl. Mater. Today, vol. 7, pp. 120–133, 2017.

[16] J. M. Hoey, A. Lutfurakhmanov, D. L. Schulz, and I. S. Akhatov, “A review on aerosol-based direct-write and its applications for microelectronics,” J. Nanotechnol., vol. 2012, 2012.

[17] OPTOMEC, “Aerosol Jet ® Printed Electronics Overview,” p. 6.

[18] S. Binder, M. Glatthaar, and E. Rädlein, “Analytical investigation of aerosol jet printing,” Aerosol Sci. Technol., vol. 48, no. 9, pp. 924–929, 2014.

[19] C. S. Alex Gong, W. J. Syu, K. F. Lei, and Y. S. Hwang, “Development of a flexible non-metal electrode for cell stimulation and recording,” Sensors (Switzerland), vol. 16, no. 10, 2016.

[20] B. Zhmud, D. Ph, and A. Prof, “Lube-Tech093-ViscosityBlendingEquations,” no. 5, pp. 2–5.